Available online at www.sciencedirect.com

SciVerse ScienceDirect

Journal of the European Ceramic Society 32 (2012) 2153–2162

www.elsevier.com/locate/jeurceramsoc

Phase metastability of nanosized α-Al_2O_3 crystallites

Rung-Je Yang [a], Pei-Ching Yu [a], Chih-Cheng Chen [b], Fu-Su Yen [a,*]

[a] *Department of Resources Engineering, National Cheng Kung University, No. 1 University Rd., Tainan 70101, Taiwan, ROC*
[b] *Department of Mechanical Engineering, Far East University, No. 49, Jhonghua Rd., Shinshih Dist., Tainan 74448, Taiwan, ROC*

Received 4 August 2011; received in revised form 15 February 2012; accepted 27 February 2012
Available online 18 March 2012

Abstract

The reversal of the α- to θ-Al_2O_3 phase transformation and the induced microstructure evolution of boehmite-derived discrete nanosized α-crystallites are examined. Three categories of α-crystallites smaller than 100 nm were examined and found to have similar behavior: (1) pre-existing α-crystallites, (2) α-crystallites formed in situ during the calcination of θ-crystallites of sizes near the critical size, 25 nm, and (3) α-crystallites formed in situ by the thermal treatment of as-received θ-crystallites. The α-crystallite may transform back to the θ-phase above 800 °C. The backwards θ-crystallite may also re-transform to the α-phase again. Because of the density difference between α- and θ-Al_2O_3, the strain involved in the volume expansion and shrinkage during the phase transition eventually results in the formation of a twinned and/or mosaic structure for the θ- and α-crystallites. A strain release model representing the microstructure evolution of the α- to θ-phase and the θ- to α-Al_2O_3 phase transformation is proposed.

Keywords: D. Al_2O_3; Phase transformation; Crystal growth; Crystallite size

1. Introduction

The nucleation and growth mechanism has been considered the elementary procedure for forming a new phase particle.[1–3] During the procedure, a critical size is required to form the nucleus of the new phase. As the nucleus continues to grow, exceeding the size at which the particle is thermodynamically stable; the volume energy, $V\Delta G_v$ grows larger than the surface energy, $S\Delta\gamma$ (the total free energy change, ΔGr, becomes negative, where $\Delta Gr = S\Delta\gamma + V\Delta G_v \leq 0$). If the particles cannot grow past this threshold and meet the requirement $\Delta Gr \leq 0$, then the particles may shrink and disappear. However, in a solid-state system, the phase shrinking-and-disappearing phenomena may not occur, especially in a new phase that resulted from a phase transformation. Though it is seldom reported, it is more likely that, the shrinking-and-disappearing phenomena can be substituted by a phase transformation back to the antecedent phase.[4–6]

α-Al_2O_3 has long been one of the most widely used industrial ceramics because of its combination of physicochemical properties such as high wear resistance, high melting point, and good thermal, chemical, and mechanical stability. However, its brittle nature limits its use in the manufacture of advanced materials and therefore imposes the limitations of its applications. Phase purity and crystallite size of the starting materials play a very important role in the fabrication of dense and fine-grained alumina ceramics and provide a pathway for overcoming the disadvantages.[7] Previous studies indicated that the transition Al_2O_3 phase coupled with the high activation energy for nucleating α-Al_2O_3 would greatly impede efforts to process dense α-Al_2O_3 with a controlled grain size, especially for submicrometer materials.[8] The nanosized α-Al_2O_3 powder currently found on the market can be composed of more than 95% of α-phase Al_2O_3 crystallites. However, these crystallites are generally approximately 150–200 nm in size and are characterized by a vermicular-growth structure. Each crystallite is a single crystal but with an outward shape formed by connecting two or more α-Al_2O_3 crystallites with diameters of approximately 100 nm.[9–11] The vermicular microstructures occurring in the green compacts will inhibit further densification of alumina ceramics. Likewise, nanosized discrete α-Al_2O_3 powder is of a lower α-phase purity, though it can be composed of α-crystallites free of vermicular-growths and is smaller than 100 nm. In other words, there is no high phase-pure discrete α-Al_2O_3 crystallite powder less than

* Corresponding author. Tel.: +886 6 2355603; fax: +886 6 2380421.
E-mail address: yfs42041@mail.ncku.edu.tw (F.-S. Yen).

0955-2219/$ – see front matter © 2012 Elsevier Ltd. All rights reserved.
doi:10.1016/j.jeurceramsoc.2012.02.044

Table 1
The specification of commercial ultrafine α-Al_2O_3 crystallite powder available on the market.

Manufacturer	Product	α-Phase fraction (wt%)	BET (m^2/g)	Average particles size (nm)
Taimei	TM-DAR	>99	13.2	190
Baikowski	CR30F	80	26	400
	CR10	98	8	450
Sasol	SPA-0.5		7.5	600
Sumitomo	AKP-3000	>99	4–8	400–700

TAIMEI Chemical Co., Ltd., Japan.
Baikowski Malakoff Inc., USA.
Sasol North American Inc., USA.
Sumitomo Chemical Co., Ltd., Japan.

100 nm in diameter available on the market at present (Table 1). In previous studies, both in the literature[8] and in experiences from research, it was found that nanosized high phase-pure α-Al_2O_3 crystallite powder was not easily obtained by thermal treatment of θ-Al_2O_3 crystallites (crystallite size ≤ 20 nm) through θ- to α-phase transformation. It was not until very recently that fabrication of such powders through core–shell techniques using boehmite (AlOOH) as the starting material was reported to be possible.[12] The α-phase Al_2O_3 particle was obtained through the nucleation and growth mechanism,[9–18] which may either be thermodynamically metastable[19–22] or stay at the state of an unfinished phase transformation if the crystallite is smaller than the dimension needed to make the volume energy, $V\Delta G_v$ larger than surface energy, $S\Delta\gamma$. Recent studies[19] show that ΔGr of α-Al_2O_3 crystallites smaller than 100 nm could be greater than 0 and the crystallites could behave as thermodynamically metastable. Thus, the nanosized α-Al_2O_3 crystallites would experience phase transformation reversal, backwards to the antecedent θ-phase if appropriate treatments were employed. The phase transformation reversal phenomena may be one of the major reasons why there is no high phase-pure discrete α-Al_2O_3 crystallite powder less than 100 nm in diameter available on the market.

Based on the concepts mentioned above, this study demonstrates the thermodynamic stability of boehmite-derived discrete α-Al_2O_3 crystallites smaller than 100 nm in diameter. It attempts to describe the phase transformation reversal phenomena through XRD examinations, as well as microstructure evolution, which occurs to Al_2O_3 crystallites when induced by density differences during the backward α- to θ- and the followed forward θ- to α-phase transformations. The densities of θ- and α-Al_2O_3 are 3.65 and 3.98 g/cm^3, respectively,[23] allowing the occurrence of backward (α- to θ-Al_2O_3) and forward (θ- to α-Al_2O_3) phase transitions to result in an 8.3% volume expansion and a 9.0% volume reduction to the Al_2O_3 crystallites, respectively. Thus, it is possible to find the necessary information from the variation in volume,[24] especially for the microstructures exhibited by the larger Al_2O_3 crystallites, using TEM techniques.

Boehmite-derived discrete α-Al_2O_3 crystallites smaller than 100 nm were used as the examination sample. The α-crystallite was obtained by thermal treatment of the θ-Al_2O_3 crystallite (crystallite size ≤ 20 nm) through the θ- to α-phase transformation.[25–27] Previous studies have demonstrated that there is a critical crystallite size ($d_{c\alpha}$ = ~17 nm, XRD-Scherrer formula on $(0\,1\,2)_\alpha$) for phase transformation[16–18] and that there can be a size limit of approximately 100 nm for the α-Al_2O_3 to be present as discrete particles.[9,12,19,28] Thus, α-Al_2O_3 powders with crystallites ranging from 20 to 100 nm in size were presumed to consist of metastable α-Al_2O_3 particles.[19] Furthermore, thermodynamically, the newly formed α-Al_2O_3 crystallites that stay at the stage of crystal growth may behave as metastable. Clearly, both would transform back to the θ-phase and thus should be examined. This study indicates that the phase transformation reversal phenomena may be one of the major reasons why it is not easy to obtain high phase-pure discrete α-Al_2O_3 crystallite powder of less than 100 nm in diameter through θ- to α-phase transformation.

2. Experimental

2.1. Sample preparations

Two categories of examination samples were used in this study.

(1) Samples for examining occurrence of the α- to θ-Al_2O_3 phase transformation: To observe the possible phase transformation reversal, a two-stage thermal treatment was employed. Firstly, commercial θ-Al_2O_3 powder (Ceralox Co., USA, Table 2) was heated at 1200 °C for 60 s in a tube furnace to intentionally produce approximately 30 wt% of incipient α-Al_2O_3 crystallites less than 100 nm in size. Thus, the powder system was composed of α- and two kinds of θ-Al_2O_3 crystallites of different sizes: (1) θ-Al_2O_3 crystallites approximately 25 nm in size, the critical size of phase transformation[16–18] and (2) substantial amounts of the remainder θ-Al_2O_3 crystallites less than 25 nm in size. The possibility of reversal of the α- to θ-Al_2O_3 phase transformation was then tested using the α- + θ-Al_2O_3 crystallite powder. After heating at 1200 °C, to prevent the incipient nanosized α-crystallites from growing, the powders (α- + θ-Al_2O_3) were subsequently moved from positions at 1200 °C to positions at 700–1000 °C in the tube furnace and then thermally treated for various durations. Particles at temperatures above 1000 °C were abandoned because of vermicular growth. It is apparent that the α-crystallites represent pre-existing crystallites that are subject to phase-transforming

Table 2
The basic physical properties of θ-Al_2O_3 powder.

θ-Al_2O_3	Phase	Crystallite size[a] (nm)	BET[b] (m^2/g)	Mean particle size[c] (nm)
	θ (δ)	20	75	50.0

[a] XRD-Scherrer formula on $(2\,0\,\bar{2})_\theta$.
[b] N_2-BET adsorption.
[c] Dynamic light scattering (Zetasizer 1000, Malvern, Germany).

back to the θ-phase or are otherwise ready for size coarsening to accomplish the θ- to α-Al_2O_3 phase transformation, depending on the heat treatment conditions. Of the two kinds of θ-crystallites, one represents those that are susceptible to transforming to α-Al_2O_3 if the kinetic conditions are satisfied. The other kind waits for sufficient energy provided by thermal treatment to continue size coarsening and then transform into α-Al_2O_3. The α-crystallites derived from the two types of θ-Al_2O_3 crystallites are formed in situ during thermal treatment and may experience phase transformation reversal to the θ-Al_2O_3 crystallite if the requirements for the size coarsening process have not been met.

(2) Samples for examining microstructure evolution: Three samples were prepared for this part, including (1) nanosized α-Al_2O_3 powder formed by the calcination of θ-Al_2O_3–boehmite agglomerates,[12] (2) θ-Al_2O_3 crystallites transformed from α-Al_2O_3, less than 100 nm in size, and (3) regenerated α-Al_2O_3 crystallites formed by the calcination of θ-Al_2O_3 crystallites transformed from nanosized α-Al_2O_3.

To prepare the agglomerates, a well dispersed θ-slurry (30 wt% solid content), in which the θ-Al_2O_3 crystallites were used as the core, was prepared by dispersing θ-Al_2O_3 powder (Table 2) in deionized water at pH 4 and was homogenized by a perl mill machine (Drais, Germany). An aqueous solution containing Al^{3+} (0.2 M) used for forming boehmite was obtained by dissolving $Al(NO_3)_3{\cdot}9H_2O$ (Merck, Germany) in deionized water. The θ-Al_2O_3 was then mixed with an $Al(NO_3)_3{\cdot}9H_2O$ solution. The mass ratio of θ-Al_2O_3 to Al_2O_3, derived from boehmite for forming the core–shell structure, was 30–70.[12] Heterogeneous precipitation of the boehmite shell on the θ-Al_2O_3 core was obtained until pH 9 was reached by adding an ammonium solution (NH_4OH, Freak, USA). The precipitates were washed three times with deionized water and then dried at 80 °C for 24 h to obtain gel fragments. The gel fragments were ground to less than 200 mesh with agate mortar and pestle. The discrete α-Al_2O_3 powder was obtained through thermal treatment of the gel fragments at 1150 °C for 5–10 min and then quenched to room temperature in the air.

The θ-Al_2O_3 crystallites, transformed from metastable α-Al_2O_3, and the regenerated α-Al_2O_3 crystallites were then obtained through calcination of discrete α-Al_2O_3 at 800° and 900 °C, respectively, for various times. All of the samples were treated in the air and quenched to room temperature (cooling rate > 250 °C/min) as the prescribed heating conditions were satisfied. Though water vapor may affect the phase transformation during heating,[29] it was uncontrolled in this study.

2.2. Characterization

Crystalline phase identifications and crystallite size measurements were performed using XRD powder methods (Rigaku, Japan) with Ni-filtered Cu *K*α radiation. The samples were scanned from (2θ=) 20° to 80° at a scanning rate of 4°/min. The mean sizes of the α-Al_2O_3 crystallites in the samples were calculated with the XRD-Scherrer formula[30] (crystallite size = $0.9\lambda/B\cos\theta$, where λ = 1.540 Å, B = the width at the half-peak height (WHPH) in radians, and θ = the Bragg angle). The reflection peak of $(0\,1\,2)_\alpha$ α-Al_2O_3 was applied. The scanning rate was 0.5°/min and 2θ was 24.5–34.5°. The instrument peak width was calibrated using a well-crystallized silicon powder. Data calculations were assisted by the following software: XRD Pattern Processing and Identification, Jade for Windows, Version 5.0, developed by Materials Data Inc. The fraction of α-Al_2O_3 formation was determined by quantitative XRD powder methods using CaF_2 as the internal standard. The integrated intensities of the (0 1 2) reflection for α-Al_2O_3 and the (1 1 1) reflection for the CaF_2 internal standard (10 wt%) were measured and the ratio was compared to an α-Al_2O_3-CaF_2 calibration curve. The range of investigation was 1.5–97 wt%. The morphology and microstructure of the θ- and α-Al_2O_3 crystallites were examined with a transmission electron microscope (TEM, JEOL AEM-3010, and Tecnai FEG-TEM).

3. Results and discussion

3.1. Reversal of the α- to θ-Al_2O_3 phase transformation

First, θ-Al_2O_3 powders were calcined at 1200 °C for 60 s to fabricate α- + θ-Al_2O_3 crystallite powder containing 20–30 wt% (~27%) α-Al_2O_3 crystallites less than 100 nm in size. The phase transformation reversal phenomena was then examined using the samples prepared by subsequently placing the α- + θ-Al_2O_3 crystallite powder at temperatures 700, 800, 900, and 1000 °C for anticipated durations after heating at 1200 °C for 60 s. The samples were then quenched to room temperature. The XRD patterns and the percentage of the α- to θ-Al_2O_3 phase transformation shown in Fig. 1 illustrate that the α- to θ-Al_2O_3 phase transformation phenomenon can be observed in the α- + θ-Al_2O_3 crystallite powder. Fig. 1(a) indicated that the XRD patterns obtained from samples calcined at 700 °C were very similar. However, the XRD patterns obtained from samples calcined at 800–1000 °C show that the intensity of the (0 1 2) diffraction peak of α-Al_2O_3 decreases while that of the $(2\,0\,\bar{2})$ diffraction peak of the θ-phase increases with the holding time of the thermal treatments. It can be concluded that the α-phase Al_2O_3

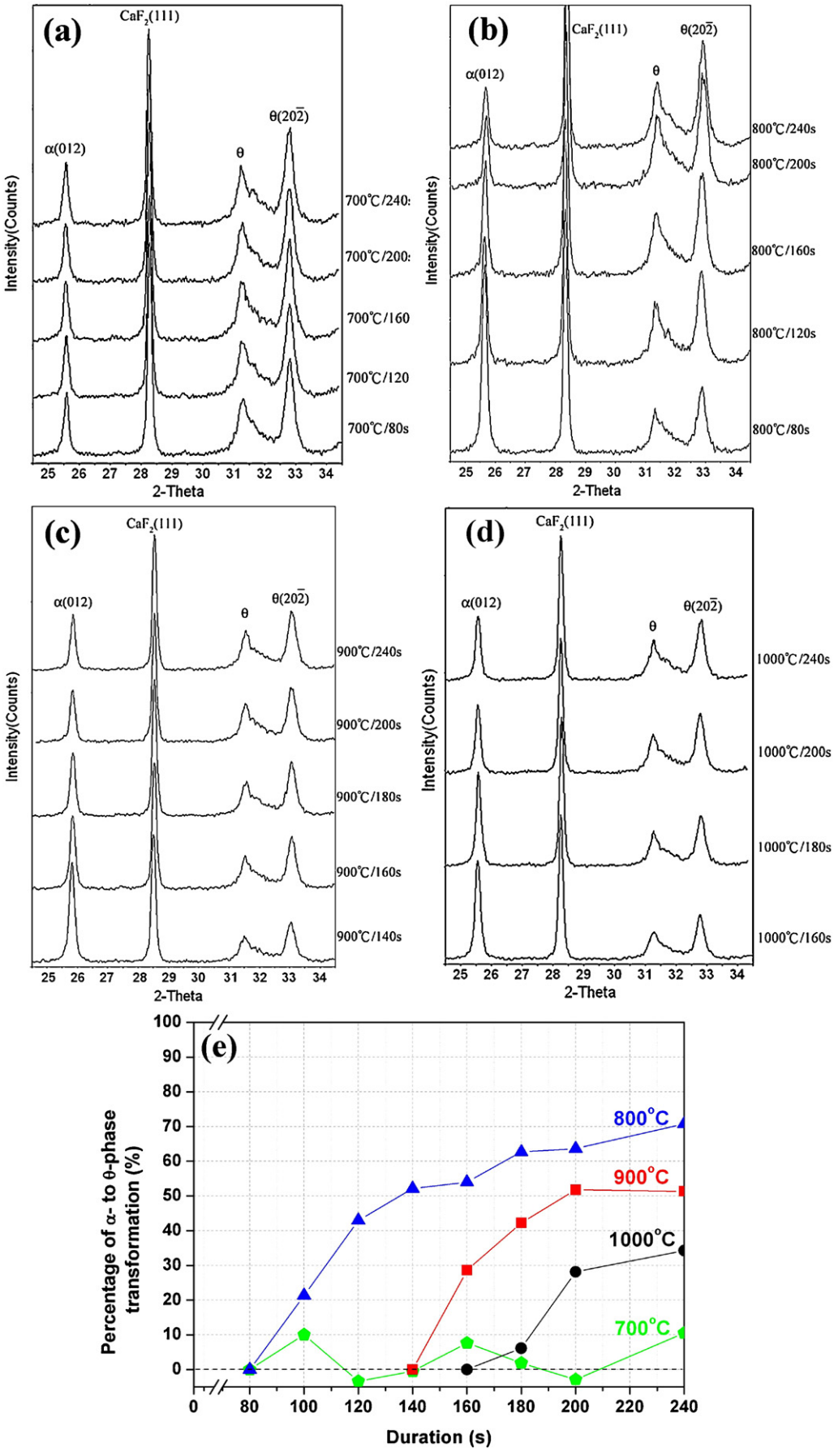
(a)
CaF2(111)
α(012)
θ
θ(20$\bar{2}$)
700℃/240s
700℃/200s
700℃/160s
700℃/120s
700℃/80s
Intensity(Counts)
2-Theta
(b)
CaF2(111)
α(012)
θ
θ(20$\bar{2}$)
800℃/240s
800℃/200s
800℃/160s
800℃/120s
800℃/80s
Intensity(Counts)
2-Theta
(c)
CaF2(111)
α(012)
θ
θ(20$\bar{2}$)
900℃/240s
900℃/200s
900℃/180s
900℃/160s
900℃/140s
Intensity(Counts)
2-Theta
(d)
CaF2(111)
α(012)
θ
θ(20$\bar{2}$)
1000℃/240s
1000℃/200s
1000℃/180s
1000℃/160s
Intensity(Counts)
2-Theta
(e)
800°C
900°C
1000°C
700°C
Percentage of α- to θ-phase transformation (%)
Duration (s)

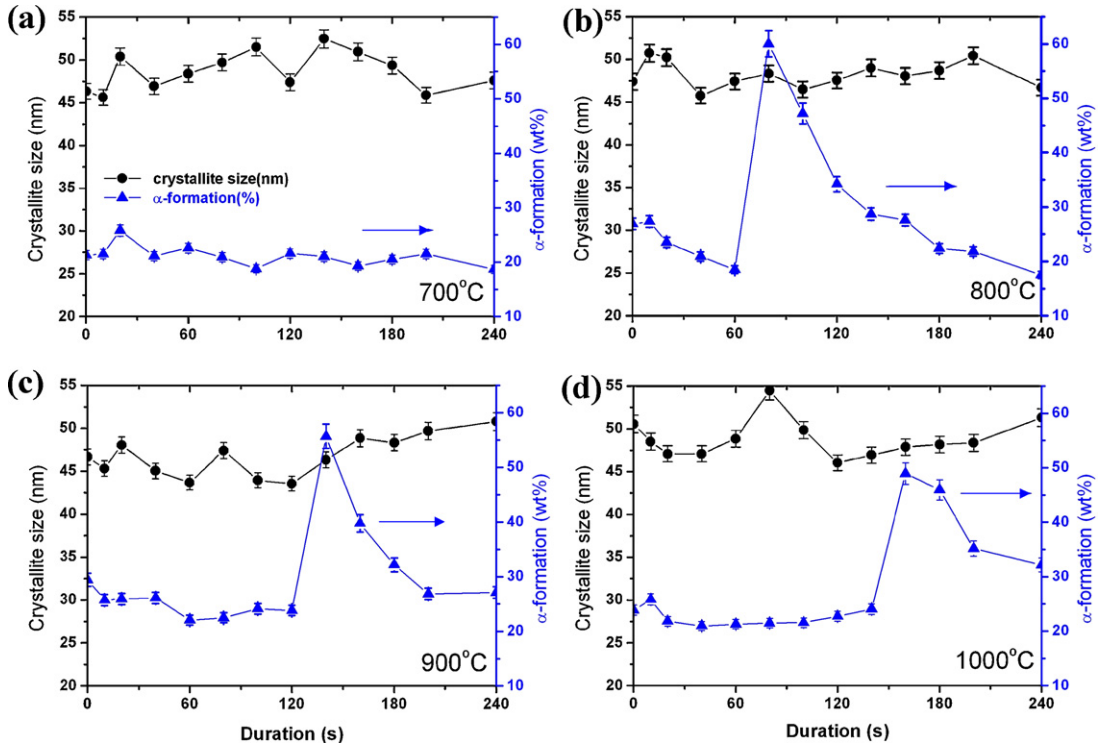

Fig. 2. Characteristics of phase transformation reversal of α-Al_2O_3 observed in α- + θ-Al_2O_3 powder systems during thermal treatment. The examined samples were thermally treated at temperatures of (a) 700 °C, (b) 800 °C, (c) 900 °C, and (d) 1000 °C. The results show that the nanosized α-Al_2O_3 crystallites experienced phase transformation reversal to the θ-phase within tens of second when the crystallites were thermally treated at temperatures above 800 °C.

crystallites could transform back to the θ-phase when calcined at temperatures around 800–1000 °C. Fig. 1(e) shows the percentage of the α- to θ-Al_2O_3 phase transformation during the thermal treatment. It shows that the maximum amount of phase transformation reversal that can be reached is 70%, 50%, and 35% at 800 °C, 900 °C, and 1000 °C, respectively. More detailed data are shown in Fig. 2 and illustrated as follows.

Fig. 2 compiles the characteristics of phase transformation reversal of α-Al_2O_3 crystallites occurring in the α- + θ-Al_2O_3 crystallite powder. The powder systems were composed of the incipient α- and a remainder of θ-Al_2O_3 crystallites equal or near to and smaller than the critical size for phase transformation (∼25 nm). As a result, the α-formation, measured from samples at specific time intervals during thermal treatment, must include both the disappearance of the pre-existing (incipient) α- and newly appeared α- that formed in situ from the remainder θ-Al_2O_3 crystallites. Furthermore, as the θ- to α-Al_2O_3 phase transformation is achieved through the nucleation and growth mechanism, θ-crystallites with larger sizes (especially those equal or near to the critical size of transformation) may convert to the α-phase faster than those with smaller sizes at the same temperature. The formation of α-Al_2O_3 in situ would occur sequentially from large θ-Al_2O_3 to small. Thus, the variation in α-Al_2O_3 formation with the holding duration shown in Fig. 2 indicates that there can be a forward and backward phase formation progressing in the powder system. Additionally, the α- to θ-Al_2O_3 phase transformation is normally accessible to the finer crystallites, leaving the coarser crystallites in the rest of the powder system. If one compared the α-size variation before and after phase transformation reversal, the latter would show coarser α-sizes. Thus, it is interesting to find that it is possible to examine phase transformation reversal based on α-Al_2O_3 formation and the accompanied α-size variation.

Fig. 2(a) indicates that the holding temperature 700 °C was too low and was thus unable to provide sufficient energy for the forward and backward phase transformation to take place, even when the holding time exceeded 240 s. When raising the temperature to 800 °C, the amount of pre-existing α-crystallites (∼27 wt%) decreased. Approximately a 37 percent reduction (10/27 = 0.37) in the pre-existing α-crystallites was observed before the newly formed α-Al_2O_3 crystallites (at 80–105 s) were formed from coarser θ-crystallites. It is clear that the duration needed to initiate phase transformation reversal of the pre-existing α-Al_2O_3 crystallite can be less than 10 s. After an 80-s holding time, more than 40 wt% (60–20 wt% as shown in Fig. 2(b), percentage reduction ∼70% (60–17.5/60 = 0.70) as

Fig. 1. The XRD patterns of α- + θ-Al_2O_3 powders thermally treated at (a) 700 °C, (b) 800 °C, (c) 900 °C, and (d) 1000 °C for various durations. (e) Percentage of the α- to θ-Al_2O_3 phase transformation observed in the powder systems during thermal treatment. The reversal of the α- to θ-Al_2O_3 phase transformation phenomena could be clearly observed as the samples were treated at (b) 800° and (c) 900 °C. The maximum amount of phase transformation reversal can reach up to 70% and 50% at 800 °C and 900 °C, respectively.

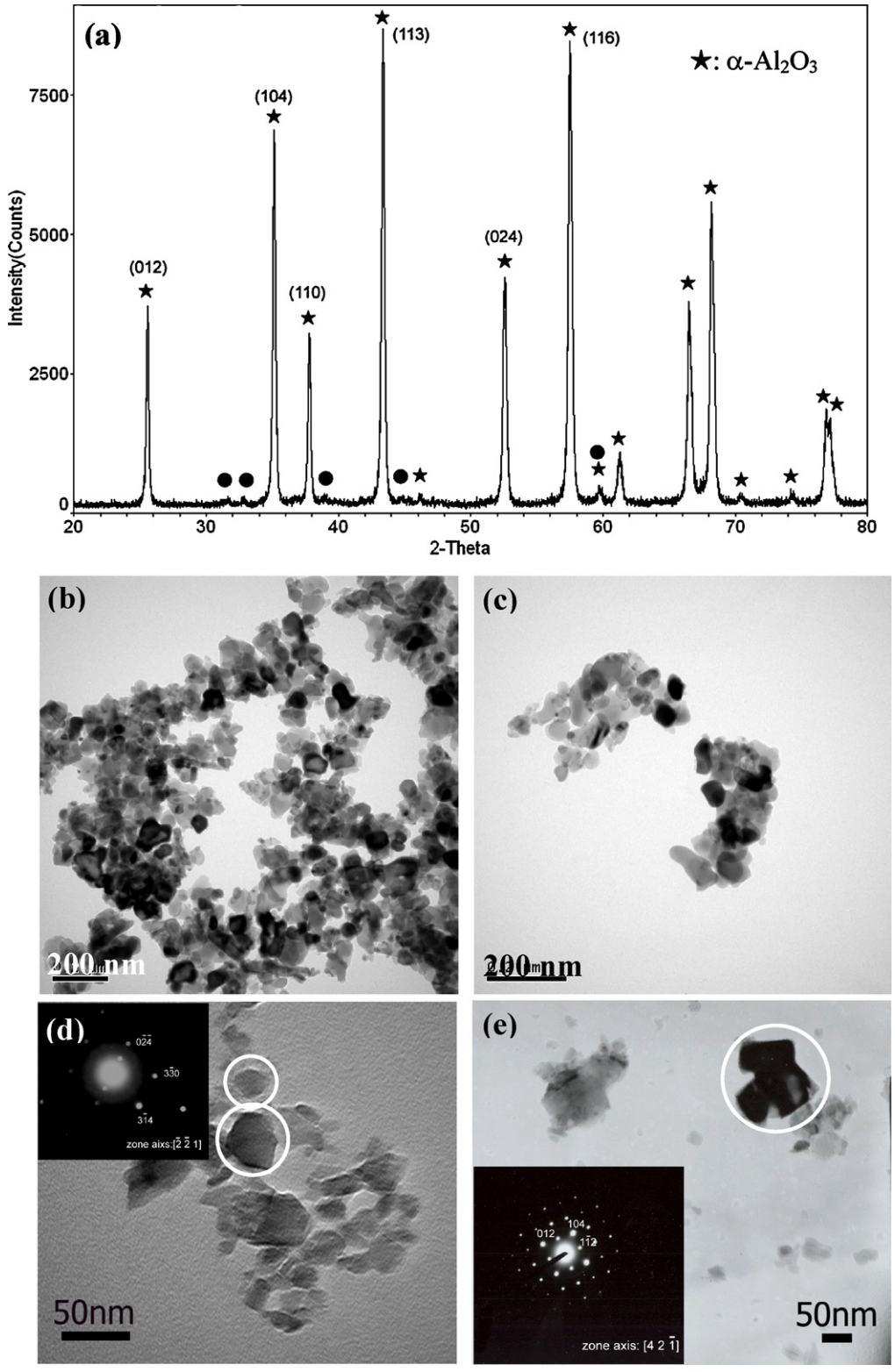

Fig. 3. Morphologies of discrete α-Al_2O_3 crystallites obtained by calcinations of α-Al_2O_3–boehmite agglomerates at 1150 °C/5 min. Typical XRD patterns (a), general views (b) and (c), and crystallites with sizes (d) ∼17 and ∼50 nm, and (e) crystallites with vermicular growth.

shown in Fig. 1(e) of the newly formed α-Al_2O_3 crystallite resulted from phase transformation of θ-crystallites occurred. As the temperature 800 °C eventually triggered the reversal of the α- to θ-Al_2O_3 phase transformation, the newly formed α-Al_2O_3 crystallites went backwards to θ-crystallites again seconds after their formation. It is noted that the rate of phase transformation reversal of the newly formed α-Al_2O_3 crystallites from coarser θ-crystallites accelerated at 900° and 1000 °C, compared

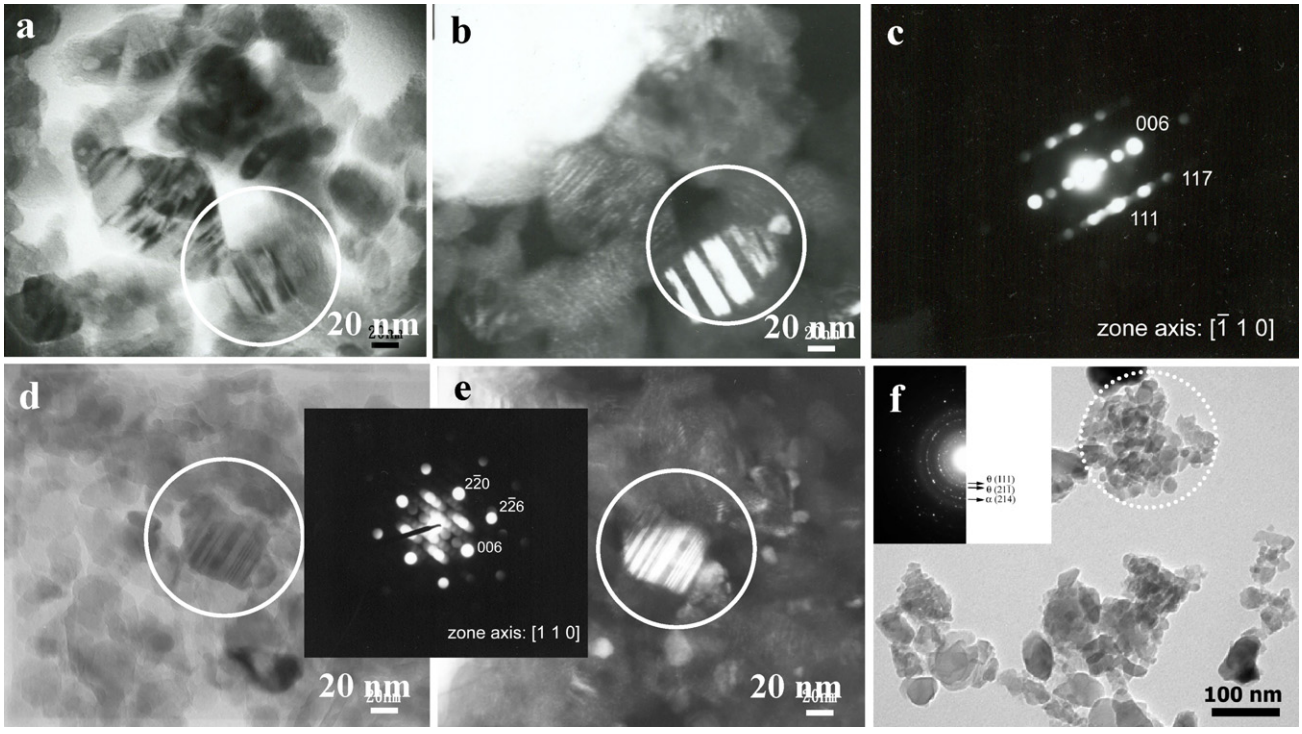

Fig. 4. (Upper a–c) Twinned θ-Al_2O_3 crystallites gained by thermally treating 50–100 nm α-Al_2O_3 crystallites. The bright-field (a) and centered-dark field images (b) of TEM micrographs and the corresponding diffraction pattern of [$\bar{1}$ 1 0] zone (twin plane: (0 0 1)) (c) of the examined sample calcined at 800 °C for 60 s. (Bottom d–f) TEM micrographs of twinned α-Al_2O_3 (d and e) drawn from metastable twinned θ-Al_2O_3 and mosaic structured α-Al_2O_3 (f).

with that seen at 800 °C. Furthermore, the amounts measured were compensated by the disappearance of pre-existing α-Al_2O_3 crystallites. This is evident from the α-size increment (Fig. 2(c) and (d) at 85–90 s). The size coarsening of smaller θ-crystallites may initiate at temperatures above 900 °C. The corresponding α-Al_2O_3 formation started after the heating duration exceeded 120 s (Fig. 2(c) and (d)). A similar situation occurred with the α-crystallite, going backward to θ-crystallites seconds after their formation. It should be noted that all α-Al_2O_3 existing at various time intervals experienced phase transformation reversal once the thermal treatment temperature exceeded 800 °C; however, higher treatment temperatures may result in size coarsening of α-Al_2O_3 which eventually may create the possibility for the crystallite to remain at α-phase state longer (Fig. 2(d)).

3.2. Morphology of nanosized α-Al_2O_3 crystallites

Fig. 3 displays the morphology of discrete α-Al_2O_3 crystallites less than 100 nm in size prepared by core (θ-Al_2O_3)–shell (boehmite) agglomerate techniques. The agglomerates were calcined at 1150 °C for 5 min and then quenched to room temperature. Measurable amounts of residual θ-Al_2O_3 were found (Fig. 3(a), XRD patterns). As a whole, the grains are free of vermicular growths and are nearly spherical (Fig. 3(b) and (c), TEM micrographs). Detailed examination found that there are some α-Al_2O_3 crystallites with sizes ranging between approximately 20 and 50 nm (Fig. 3(d)). Previous studies propose that there can be two-staged growth, 17–20 and 45–50 nm, for the formed α-Al_2O_3 crystallites before the completion of phase transformation.[16,17,19] The vermicular growth would develop as the size of α-Al_2O_3 crystallites grew past approximately 100 nm (Fig. 3(e)).

The θ-Al_2O_3 crystallites obtained by phase transformation reversal of nanosized discrete α-Al_2O_3 crystallites may have grains exhibiting polysynthetic twins,[31–33] especially for the olive-like larger-sized grains (Fig. 4(a)–(c)). Previous studies[14–17] indicated that there can be a critical size of θ-Al_2O_3 crystallites during θ- to α-Al_2O_3 phase transformation. The critical size is approximately 25 nm (XRD-Scherrer formula on $(2\,0\,\bar{2})_\theta$ of θ-Al_2O_3). As θ-Al_2O_3 crystallites grow to this size, α-Al_2O_3 phase formation is triggered. According to these reports, θ-Al_2O_3 crystallites of sizes larger than 25 nm should not exist in powders. Therefore, the twinned θ-Al_2O_3 crystallites that occur in this study may be attributed to the α- to θ-phase transformation because the θ-size was larger than the critical size of θ-Al_2O_3. Multiple twinned θ-Al_2O_3 crystallites were reported previously,[32,33] although neither the size nor the formation mechanism of the twinned crystallite was discussed. However, because γ- or δ-Al_2O_3 crystallites with sizes larger than 20–25 nm have not been found so far, there can be an additional possibility of forming twined θ-Al_2O_3 crystallites, that can be originated form the reversal of the α- to θ-phase transformation. The multiple twinned lamellae are arranged along the [0 0 1] direction with (0 0 1) as the twin plane.

The α-Al_2O_3 crystallites converted from the θ-Al_2O_3 crystallites derived from phase transformation reversal may contain grains with twinned or mosaic structures (Fig. 4(d)–(f)). Obviously, due to the critical size phenomena, it is possible to find that there can be fragments of α- and θ-Al_2O_3 particles composed in a mosaic (Fig. 4(f)).

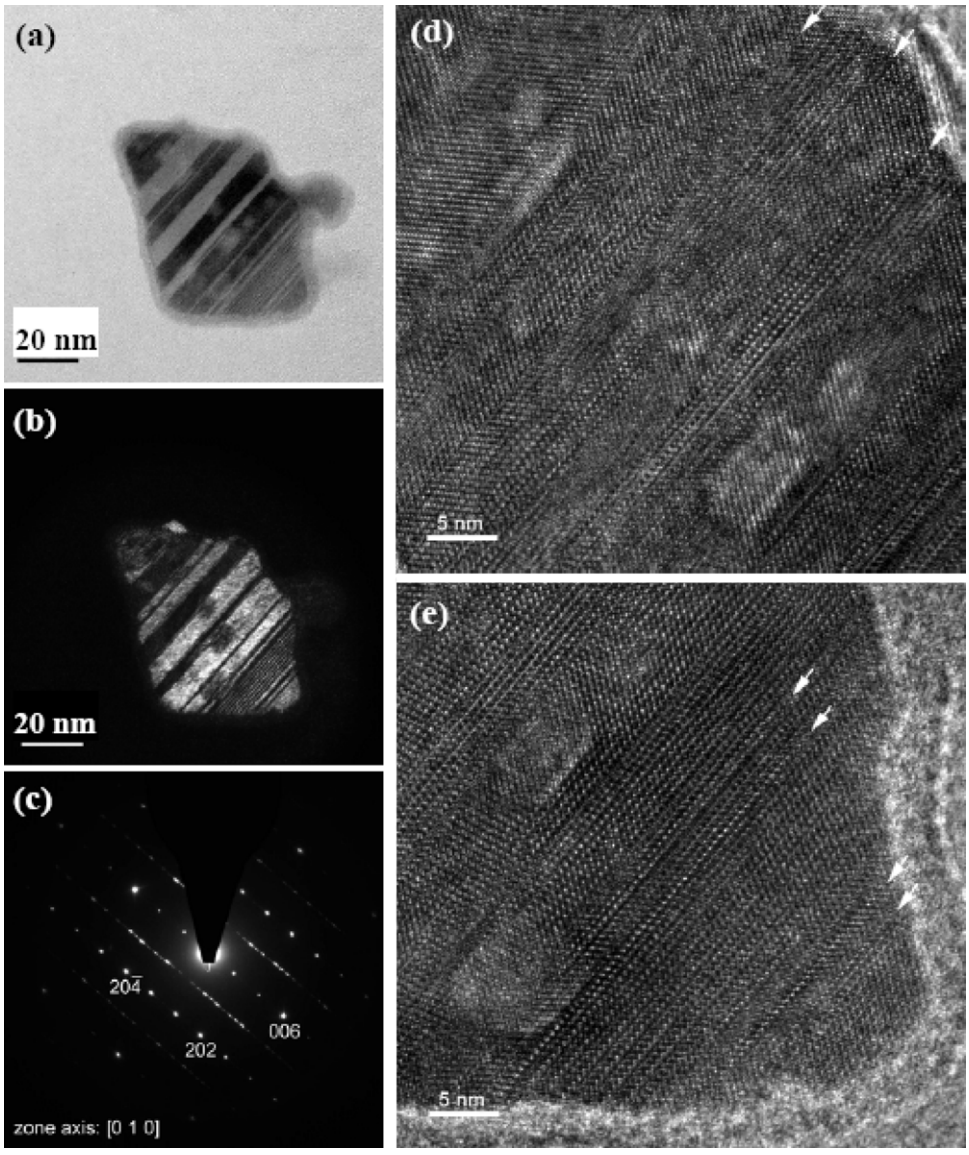

Fig. 5. (a) The bright field and (b) dark field images of TEM micrographs of θ-Al_2O_3 crystallites with twin structure, and (c) the corresponding diffraction pattern of [0 1 0] zone (twin plane: (0 0 1)). (d and e) The HRTEM images of twinned θ-Al_2O_3 crystallites in (a) showing twin boundaries (indicated by white arrows).

3.3. Microstructure evolution

It is clear that the nanosized discrete α-Al_2O_3 crystallites may undergo phase transformation reversal to θ-phase with polysynthetic twins (Fig. 4(a)–(c)) and may convert backward to α-phase again with twin and mosaic structure. The phenomenon is explained as a result of the difference in density between the two phases, equaling 3.65 and 3.98 g/cm^3 for θ- and α-Al_2O_3 phases, respectively. The occurrence of α- to θ-Al_2O_3 phase transformation can result in an 8.3% volume expansion in the crystallite. Similarly, a 9.0% volume reduction will be induced during the progression of a θ- to α-phase transformation. Therefore, the formation of the twin structure can be ascribed to as the reflection of eliminating the mechanical strain due to volume expansion. Because the twin structure was formed to eliminate the mechanical stress, the width and number of the twin lamellae can be affected by the amount of stress.[34] In this study, the lamellae generally show widths of 5–20 nm. Moreover, twin lamellae generated in one twinned crystallite could show different widths. Some lamellae even had widths smaller than 5 nm (Fig. 5). Similar characteristics of twinned θ-Al_2O_3 crystallites obtained by dehydration of boehmite at approximately 1200 °C for 3 h were reported.[32] The lamellae showed different widths but were all less than 10 nm. The twin structure can be preserved during the re-transformation of θ- to α-phase if the mechanical strain induced by volume reduction can be effectively released (Fig. 4(d) and (e)). Or the volume reduction could lead to the cracking of the α-Al_2O_3 crystallite, bringing approximately the formation of a mosaic structure (Fig. 4(f)). Further, due to the critical size phenomena, the mosaic structure would be composed of small θ- and α-Al_2O_3 fragments.

A strain release model is proposed to illustrate the microstructure evolution during the phase stabilization process of the metastable α-Al_2O_3 crystallite in this study (Fig. 6). At first, the

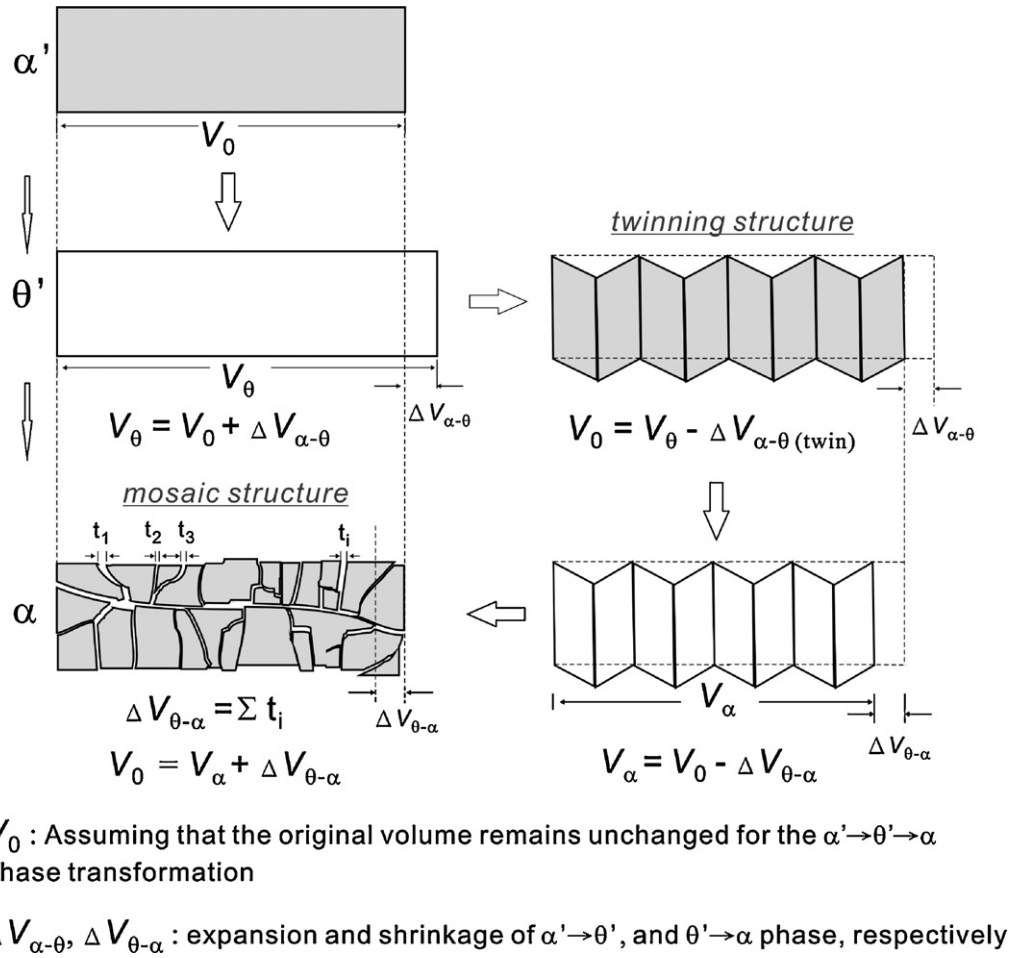

Fig. 6. Strain release model for phase stabilization of nanosized α-Al_2O_3 crystallites.

volume expansion induced by the reversal of the α- to θ-phase transformation results in the θ′-Al_2O_3 crystallites with a twin structure. As the θ′-crystallites may retransform to the α-phase, the twin structure can either be preserved or the mosaic structure will be created, depending on the effectiveness of releasing the mechanical strain.

4. Conclusions

Discrete α-Al_2O_3 crystallites smaller than 100 nm in size of the pre-existing type and those obtained in situ during thermal treatment, including from θ-Al_2O_3 crystallites of sizes near to and smaller than the critical size of phase transformation were examined to have similar reversal of phase transformation behavior.

1. The nanosized α-Al_2O_3 crystallites experienced phase transformation reversal to the θ-phase within tens of second when the crystallites were thermally treated at temperatures above 800 °C. The backward θ-phase crystallite may transform to the α-phase again if the appropriate thermal treatment conditions were adopted.
2. The phase transformation reversal of α- to θ- and the reconversion of θ- to α- is evident from the presence of twinned θ- and twinned or mosaic α-Al_2O_3 crystallites, respectively. A strain release model is proposed in this study.

This study indicates that the phenomena of the reversal of phase transformation may be one of the major reasons why there is no high phase-pure discrete α-Al_2O_3 crystallite powder less than 100 nm in diameter available on the market.

Acknowledgments

The authors would like to thank Miss Hsiu-Wen Chen for her assistance with the experiments and Miss Liang-Chu Wang of National Sun Yat-Sen University for her assistance in the TEM examinations. This study was supported by the National Science Council (NSC – 93-2216-E-006-042) and the Ministry of Economic Affairs (93-EC-17-A-08-S1-023) of the Republic of China.

References

1. Mullin JW. *Crystallization*. 2nd ed. London: Butterworths; 1972.
2. Volmer M. *Kinetic der Phasenbildung*. Dresdem, Germany: Steinkoff; 1939.
3. Putnis A. *Introduction to mineral sciences*. New York: Cambridge University Press; 1992.

4. Gary M, McAfee Jr R, Wolf CL. *Glossary of geology*. Washington, DC: American Geological Institute; 1987. p. 604–5.
5. Zhang H, Banfield JF. Understanding polymorphic phase transformation behavior during growth of nanocrystalline aggregates: insights from TiO_2. *J Phys Chem B* 2000;**104**:3481–7.
6. Zhu KR, Zhang MS, Hong JM, Yin Z. Size effect on phase transition sequence of TiO_2 nanocrystal. *Mater Sci Eng A* 2005;**403**:87–93.
7. Mayo MJ. Processing of nanocrystalline ceramics from ultrafine particles. *Int Mater Rev* 1996;**41**:85–115.
8. Laine RM, Marchal JC, Sun HP, Pan XQ. Nano-α-Al_2O_3 by liquid-feed flame spray pyrolysis. *Nat Mater* 2006;**5**:710–2.
9. Badker PA, Bailey JE. The mechanism of simultaneous sintering and phase transformation in alumina. *J Mater Sci* 1976;**11**:1794–806.
10. Dynys FW, Halloran JW. Alpha alumina formation in alum-derived gamma alumina. *J Am Ceram Soc* 1982;**65**:442–8.
11. Dynys FW, Halloran JW. Alpha alumina formation in Al_2O_3 gels. In: Hench LL, Ulrich DR, editors. *Ultrastructure processing of ceramics, glasses and composites*. New York: John Wiley and Sons; 1984. p. 142–51.
12. Yu PC, Yang RJ, Chang YT, Yen FS. Fabrication of nano-scaled α-Al_2O_3 crystallites through heterogeneous precipitation of boehmite in a well-dispersed θ-Al_2O_3-suspensions. *J Am Ceram Soc* 2007;**90**:2340–6.
13. Messing Bagwell RB, Howell GLPR. The formation of α-Al_2O_3 from θ-Al_2O_3: the relevance of a "critical size" and: diffusional nucleation or "synchro-shear"? *J Mater Sci* 2001;**36**:1833–41.
14. McArdle JL, Messing GL. Seeding with γ-alumina for transformation and microstructure control in boehmite-derived α-alumina. *J Am Ceram Soc* 1986;**69**:c-98–101.
15. McArdle JL, Messing GL. Transformation, microstructure development, and densification in α-Fe_2O_3-seeded boehmite-derived alumina. *J Am Ceram Soc* 1993;**76**:214–22.
16. Wen HL, Chen YY, Yen FS, Huang CY. Size characterization of θ- and α-Al_2O_3 crystallites during phase transformation. *Nanostruct Mater* 1999;**11**:89–101.
17. Wen HL, Yen FS. Growth characteristics of boehmite-derived ultrafine theta and alpha-alumina particles during phase transformation. *J Cryst Growth* 2000;**208**:696–708.
18. Chang PL, Yen FS, Cheng KC, Wen HL. Examinations on the critical and primary crystallite sizes during θ- to α-phase transformation of ultrafine alumina powders. *Nano Lett* 2001;**1**:253–61.
19. Yang RJ, Yu PC, Chen CC, Yen FS. Growth thermodynamics of nanoscaled α-alumina crystallites. *Cryst Growth Des* 2009;**9**:1692–7.
20. McHale JM, Auroux A, Perrotta AJ, Navrotsky A. Surface energies and thermodynamic phase stability in nanocrystalline aluminas. *Science* 1997;**277**:788–91.
21. Lodziana Z, Parlinski K. Dynamical stability of the α and θ phases of alumina. *Phys Rev B* 2003;**67**, 174106-1–7.
22. Wolverton C, Hass KC. Phase stability and structure of spinel-based transition aluminas. *Phys Rev B* 2000;**63**, 024102-1–16.
23. Wefers K. Bell GM. *Oxides and hydroxides of alumina*. Technical Paper No. 19, Alcoa Research Laboratories; 1972.
24. Chan CC, Kriven WM, Young JF. Physical stabilization of the $\beta \rightarrow \gamma$ transformation in dicalcium silicate. *J Am Ceram Soc* 1992;**75**:1621–7.
25. Yen FS, Wang MY, Chang JL. Temperature reduction of during θ- to α-phase transformation induced by high-pressure pretreatments of nano-sized alumina powders derived from boehmite. *J Cryst Growth* 2002;**236**: 197–209.
26. Yu PC, Yen FS, Lin TC. θ-Crystallite growth restraint induced by the presence of α-crystallite in a nano-sized alumina powders system. *J Cryst Growth* 2004;**265**:137–48.
27. Yang RJ, Yen FS, Lin SM, Chen CC. Microstructure-controlled effects on temperature reduction of α-Al_2O_3 crystallite formation. *J Cryst Growth* 2007;**299**:429–35.
28. Yang Y, Wu YC, Yong L, Ping C. Preparation of ultrafine α-Al_2O_3 powder by thermal decomposition of AACH at low temperature. *Chin J Process Eng* 2002;**2**:325–9.
29. Bagwell RB, Messing GL. Effect of seeding and water vapor on the nucleation and growth of α-Al_2O_3 from γ-Al_2O_3. *J Am Ceram Soc* 1999;**82**:825–32.
30. Cullity BD. *Elements of X-ray diffraction*. 2nd ed. London: Addison-Wesley Publishing Company Inc.; 1978. p. 81–106.
31. Klein C, Hurlbut Jr CS. *Manual of mineralogy*. 21st ed. New York: John Wiley & Sons Inc.; 1993.
32. Wang YG, et al. Twinning in θ alumina investigated with high resolution transmission electron microscopy. *J Eur Ceram Soc* 1998;**18**:299–304.
33. Levin I, Brandon D. Metastable alumina polymorphs: crystal structures and transition sequences. *J Am Ceram Soc* 1998;**81**:1995–2001.
34. Arlt G. Review twinning in ferroelectric and ferroelastic ceramics: stress relief. *J Mater Sci* 1990;**25**:2655–66.